Electronic compressibility of gapped bilayer graphene

A. F. Young,[1] C. R. Dean,[2,3] I. Meric,[2] S. Sorgenfrei,[2] H. Ren,[1]
K. Watanabe,[4] T. Taniguchi,[4] J. Hone,[3] K. L. Shepard,[2] and P. Kim[1]

[1]*Department of Physics, Columbia University, New York, New York 10027, USA*
[2]*Department of Electrical Engineering, Columbia University, New York, New York 10027, USA*
[3]*Department of Mechanical Engineering, Columbia University, New York, New York 10027, USA*
[4]*Advanced Materials Laboratory, National Institute for Materials Science, 1-1 Namiki, Tsukuba, 305-0044, Japan*

(Dated: April 11, 2018)

We report on a zero magnetic field capacitance and transport study of dual gated bilayer graphene. The measured capacitance allows us to probe the electronic compressibility, or "quantum capacitance" C_Q, as a function of carrier density n, temperature, and applied perpendicular electric displacement $\overline{D}$. At $\overline{D} = 0$, C_Q decreases with density, reaching a finite minimum at $n = 0$. As the interlayer asymmetry is broken with a large $\overline{D}$, this minimum becomes deeper but remains finite, suggesting the formation of a band gap populated by disorder-induced localized states. At the edge of the gap, we observe a sharp increase in C_Q. This corresponds to the van Hove singularity expected for gapped bilayer graphene, and allows us to estimate the size of the energy gap.

PACS numbers: 81.05.ue,73.22.Pr,72.80.Vp

The unique band structures of mono- and bilayer graphene [1] (MLG and BLG) offer unprecedented tunability in a high quality two dimensional electron system (2DES). Within the independent electron approximation, intrinsic MLG and BLG are both gapless, chiral systems, with linear and hyperbolic low energy band dispersions relations, respectively. The absence of a gap presents a problem both for the use of graphenic systems in conventional electronics as well as for the realization of quantum dots and quantum point contacts, which benefit from the ability to selectively deplete regions of a 2DES. Whereas in the monolayer a gap can be opened only by a potential modulation on the spatial scale of the lattice constant[2], in BLG the sublattices are located on different layers, allowing a gap to be induced by a modulation of the interlayer imbalance *via* the application of an electric field perpendicular to the sample [3–5]. Although this field-effect tunable gap has been observed optically [6–8], conductance measurements [9] show hopping conductivity at low temperatures, suggesting the importance of localized states to conduction in substrate supported bilayer graphene.

In a parallel plate capacitor made up of imperfect conductors, adding charge n to the plates costs the sum of the classical electrostatic energy, the kinetic energy due to the resulting change in the Fermi energy, and the potential energy of Coulomb interactions between the charge carriers. The measured differential capacitance, $\delta C = \delta n/\delta V_G$, in such a system reflects this finite electronic compressibility by manifesting a lowered effective capacitance,

$$\delta C = \left(\frac{1}{C_T} + \frac{1}{C_Q}\right)^{-1} + C_P + \mathcal{O}\left(\frac{C_B}{C_T}\right) \qquad (1)$$

where $C_{T(B)}$ is the classical geometric capacitance between top (back) gate and graphene, C_P is any stray

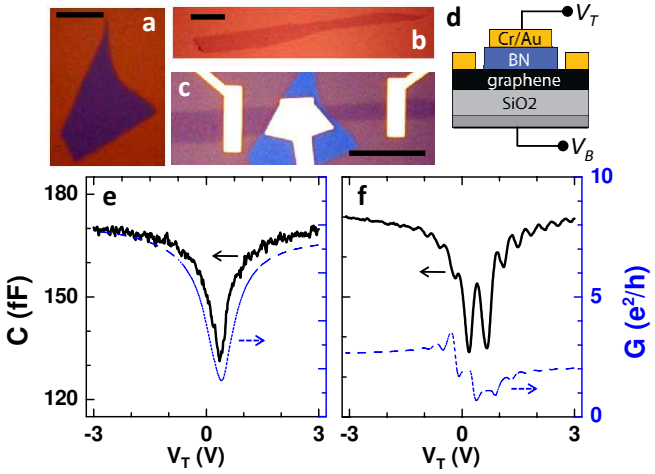

FIG. 1. A single crystal h-BN flake (a) is transferred onto mono- or bilayer graphene (b) and contacts deposited using electron beam lithography (c). Black bars are 10 μm. (d) Device schematic. (e-f) Capacitance (black,solid) and two terminal conductance (blue, dashed) of monolayer graphene at B =0 (e) and $B = 8.9$ T (f).

parallel capacitance, and $C_Q = Ae^2 dn/d\mu$ is termed the "quantum capacitance" [10], where A and μ are the area and chemical potential of the sample, respectively. In low dimensional systems C_Q can be small even when the conductivity remains large, providing an powerful tool in the study of both one [11] and two [12–17] dimensional electronic systems. Capacitance measurements are particularly powerful in the study of disordered systems, as they are able to detect localized states whose contribution to transport is suppressed.

In this Letter, we show capacitance and transport data from dual-gated bilayer graphene samples. Using Eq. 1 we extract the quantum capacitance as a func-

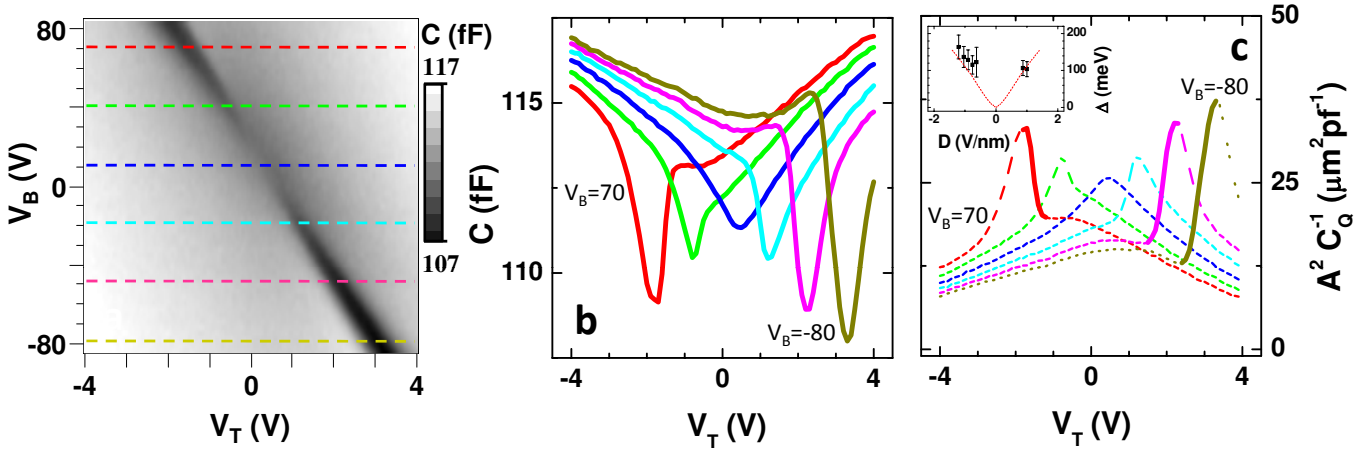

FIG. 2. (a-b) Capacitance at B=0 and 1.7 K as a function of V_T and V_B. Colored traces in (b) are taken at 30 volt intervals in V_B, corresponding to the colored lines in (a). (b) Inverse compressibility extracted from the data shown in (a-b), using C_P=1 fF for all curves. Inset: Estimation of the energy gap $\Delta = \int \frac{d\mu}{dn} dn$ found by integrating the curves over the domains of integration shown in the main panel by the solid lines. Solid red line is the band gap resulting from self consistent tight binding calculations and infrared spectroscopy on similar devices [7].

tion of temperature, density, and electronic displacement $\overline{D} = \frac{\epsilon_B}{d_B}\left(\left(V_B - V_B^0\right) - \frac{C_T}{C_B}\left(V_T - V_T^0\right)\right)$, where ϵ_B and d_B are the dielectric constant and depth of the back gate dielectric layer, $V_{T(B)}$ is the applied voltage to the top (back) gate, and $V_{T(B)}^0$ is the voltage offset required to obtain minimal density and displacement in the top gated region. Our main conclusions are as follows. At $\overline{D}$=0, C_Q reaches a minimum at n =0 and is monotonically increasing with $|n|$. With the application of a perpendicular electric field, the induced band gap manifests as a deepening of the n=0 minimum. This minimum remains finite due to the presence of disorder, which smears the band edge and induces long tails of localized states [18] throughout the energy gap. At the largest displacements applied ($\overline{D}$ >1 V/nm), local maxima in C_Q are observed, corresponding to disorder broadened van Hove singularities in the density of states, which result from the gapped bilayer energy spectrum [19, 20].

To produce dual gated graphene devices with high geometric capacitance, we utilize a single crystal hexagonal boron nitride (h-BN) [21, 22] gate dielectric. The detailed device fabrication process using h-BN will be published elsewhere [23]. Briefly, both graphene and single crystal h-BN, an insulating isomorph of graphite, are exfoliated onto n-Si/SiO_2 wafers (Fig. 1a-b). A thin (5-7 nm) h-BN flake is transferred on top of the graphene using a wet etch process and micromechanical manipulation [24], followed by electron beam lithography to form contact electrodes and a local top gate. The heavily doped silicon substrate, coated with 285 nm oxide, serves as back gate. We find that h-BN is an excellent gate dielectric, with $\varepsilon \sim$ 3-4 and breakdown fields comparable ($\sim$.8 V/nm) to SiO_2 thin films. In addition, we observe minimal degradation of graphene samples, with no additional doping contributed by the presence of the top gate and typical post h-BN transfer mobilities of $\mu \sim$5000-10,000 cm^2/V sec for graphene monolayers (see Fig. 1 c) and $\mu \sim$2000-3,000 cm^2/V sec for bilayers for SiO_2 supported samples.

Low temperature capacitance measurements were performed using a home built capacitance half-bridge similar to that used in [11]. All wires were shielded, and the sample package was encased in a Faraday cage to further reduce C_P. A ceramic multilayer capacitor (Johanson Technology 0603/R14S) with minimal temperature dependence was chosen for the reference capacitor and connected near the sample at low temperature. The noise level of the bridge was $\sim$25 $e/\sqrt{Hz}$, allowing sub-femtofarad resolution with averaging times of less than 30 seconds for our typical top gate excitation voltage of 15-50 mV. For the variable temperature capacitance measurements, we applied a 50 mV AC excitation voltage on top of the DC gate bias and measured the current through the graphene device. Although this method results in higher noise than the bridge measurement, it eliminates temperature dependent calibration errors steming from the temperature dependence of the reference capacitor. Fig. 1e-f shows the measured capacitance C and conductance G of SLG as a function of top gate voltage V_{TG} at both zero and high magnetic fields. The compressibility of SLG can be inferred from a depression at zero density, while at high B the formation of the n =0 Landau level (LL) leads to a peak at charge neutrality [17]. The high magnetic field capacitance traces show compressibility oscillations due to the formation of higher LLs, while conductance shows the electron-hole asymmetry that is the signature of edge state transport in graphene heterojunctions [25–27].

We now discuss capacitance measurements of BLG.

Fig. 2a shows the capacitance of a BLG sample at 1.7 K measured with the cold bridge. Eq. 1 allows us to convert capacitance to compressibility given C_T and C_P. We determined C_T from the device area and the ratio of the back and top gate capacitances, measured by tracking the charge neutrality point in the V_T-V_B plane (see inset to Figs. 2a and 4a). For the BLG device presented in this paper, we measured A =31 μm^2 from optical microscope images and C_T/C_B =29.5±.4, where C_B = 115 aF/μm^2 is the geometric capacitance of the back gate. Unlike the clean semiconductors [11, 12], BLG cannot be turned off completely, and, as a consequence, C_P cannot be measured directly *in situ*. Considering that the effects of interactions and disorder are most likely to be negligible at high density, we determine C_P by matching C to a clean tight binding model at the highest density measured, $n \simeq 1.5\times10^{13}$ cm^{-2}. The estimated C_P=16±1 fF, constitutes about 10% of the total capacitance signal. This value was then compared to a lower bound for the background capacitance obtained after removal of the graphene through an oxygen plasma etch, confirming the plausibility of the fit. Due to the subsequent subtraction of the (series) geometric capacitance C_T, the error introduced by fitting C_P is least important when the capacitance differs considerably from the geometric value. This is the regime in which we perform a quantitative analysis of the compressibility of gapped BLG.

Fig. 2b shows the extracted inverse compressibility $e^{-2}d\mu/dn = C_Q^{-1}$ as a function of V_T at fixed V_B. At $\overline{D} \approx 0$, C_Q^{-1} exhibits a broad maximum at n =0 as expected from compressibility of ungapped BLG. As $|\overline{D}|$ increases, C_Q^{-1} develops increasing peak values, corresponding gap-formation in the energy spectrum. We also note that there is a distinct local minimum developed at the foot of the peak. Both the peak and local minimum in C_Q^{-1} at high $|\overline{D}|$ can be understood from the single particle density of states of gapped BLG.

Within the nearest-neighbor tight binding approximation, the energy spectrum of pristine, Bernal stacked bilayer graphene with finite interlayer asymmetry Δ is given by [5]

$$\epsilon_\Delta(k) = \pm\sqrt{\frac{\gamma_1^2}{2} + \frac{\Delta^2}{4} + \epsilon_k^2 - \sqrt{\frac{\gamma_1^4}{4} + \epsilon_k^2\left(\gamma_1^2 + \Delta^2\right)}} \quad (2)$$

where $\epsilon_k = \hbar v_F k$ is the band dispersion of MLG, and γ_1 is the coupling between the dimerized A sites on one layer and $\tilde{B}$ sites on the other. This spectrum has a a "Mexican hat" structure, with the band minimum occurring at finite k_0 such that $\epsilon_{k_0} \sim \Delta/\sqrt{2}$, leading to $n \sim \sqrt{\epsilon}$ and a square-root van Hove singularity (vHs) in the density of states at the band edge. The energy scale of the "Mexican hat" is small, $\epsilon_m \sim \Delta^3/4\gamma_0^2 \lesssim 5$ meV for the gap sizes probed in this Letter, raising the question of whether such effects are robust in the presence of disorder and inhomogeneity [17]. However, even in the presence of strong disorder, the absence of a positive quadratic term in Eq. 2 turns the problem of gapped, disordered bilayer graphene into one of a heavily doped semiconductor with quartic energy bands [20]. We thus expect a $\nu \propto \epsilon^{-1/2}$ vHs-like feature to be present even in our strongly disordered ($\mu \sim$2,000 cm^2/V sec) samples.

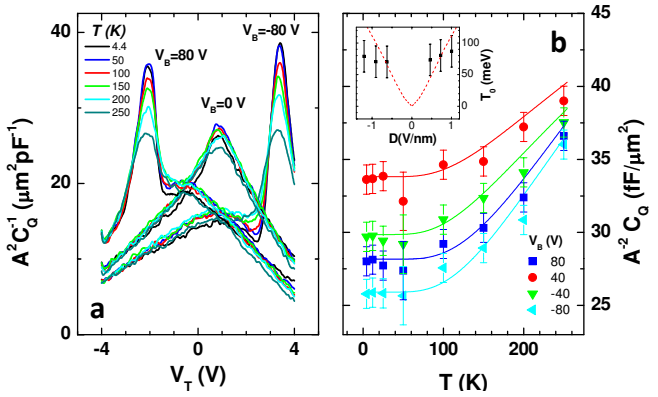

FIG. 3. (a) Temperature dependence of C_Q^{-1} for V_B = 80, 0 and -80 V. (b) Temperature dependence of the minimal compressibility C_Q(n=0). Curves were fit with a simply activated temperature dependence, $C_Q(T) = C_Q(T = 4.4K) + C_Q^T e^{-T_0/T}$, where C_Q^T and T_0 are left as free fitting parameters. A single value of C_P is chosen for all gate voltages, but is allowed to vary with temperature in order that the curves should match at high density; in all cases it is <20 fF. Inset: values of the fitting parameter T_0 as a function of $\overline{D}$. Solid line is the same as in Fig. 2b (inset).

Interestingly, the minimum associated with the vHs is only present on one edge of the band, appearing on the electron side for $\overline{D} > 0$ and the hole side for $\overline{D} < 0$. This asymmetry may be caused either by (i) inhomogenous coupling of the top gate to the graphene due to physical residues or ripples in the graphene itself or (ii) asymmetric charging of the top and bottom layers of the BLG. In scenario (i), inhomogeneity in C_T would lead to averaging over a greater density range at larger applied top gate voltages, preferentially smearing out any sharp features at higher $|V_G|$. In order to rule out (i) as the cause of the asymmetry, we fabricated top gated devices using a resist free shadow mask deposition as well as seeded atomic layer deposition HfO_2 growth [28]; we found the asymmetry to be identical in all devices measured independent of the details of the fabrication process. In scenario (ii), the interlayer screening in BLG plays an important role due to the measurement geometry, which preferentially measures the density of the layer nearer to the top gate. This suggests the possibility of quantitatively measuring the interlayer screening by careful comparison of capacitance and penetration field [12] measurements.

The observation of even the single vHs maximum in the capacitance allows us to estimate (Fig. 2b, inset) the gap in the spectrum by integrating the measured compressibility from the gap center to the density at which

the vHs occurs (solid curves in Fig. 2b),

$$\Delta \simeq 2\int_0^{n_{vHs}} \frac{d\mu}{dn} dn, \qquad (3)$$

yielding gaps of order ∼100 meV at $\overline{D}$ ∼1, in agreement with infrared spectroscopy results [7, 8]. This estimate is confirmed by temperature dependent capacitance measurements (Fig. 3). Near overall charge neutrality at $|\overline{D}| \gg 0$, our samples show a hopping conductivity similar to that observed in [9] from 1 K to ∼ 150 K. Capacitance, in contrast, shows no significant temperature dependence up to 50 K, thereafter following a simply activated dependence (Fig. 3b). This activated dependence is consistent with the presence of disorder-induced tails in the density of states throughout the band gap, and allows us to obtain an independent estimate of the gap between the effective band edges by measuring the onset of activation. This estimate, shown in the inset to Fig. 3b, is in qualitative agreement with both infrared spectroscopy and the low temperature result.

In contrast to the low density gapped regime, high density BLG devices show a weak temperature dependence of the conductivity which can be either insulating or metallic (Fig. 4). The crossover between this high density regime and the hopping regime allows us to estimate the position of mobility edge (marked by an arrow in Fig. 4 inset). We find the temperature dependence of the resistance to become exponential at slightly lower absolute density than the vHs feature in C_Q, in accordance with theoretical expectations that disorder induces states with large localization length at energies within the original band gap.

In conclusion, we have measured the capacitance of BLG and extracted the electronic compressibility. We observe the formation of an electric field induced gap and its accompanying square root vHs, albeit heavily modified by the presence of disorder. Similar measurements on cleaner samples will elucidate the role of many-body effects[29, 30] in BLG in the future.

The authors acknowledge discussions with I.L. Aleiner, B.L. Altshuler, E.A. Henriksen, J.P. Eisenstein, K.F. Mak, E. McCann, L.S. Levitov, and A.H. MacDonald. This work is supported by AFOSR MURI, FCRP through C2S2 and FENA, NRI, INDEX, DARPA CERA, NSEC (No. CHE-0117752) and NYSTAR. Sample preparation was supported by the DOE (DE-FG02-05ER46215).

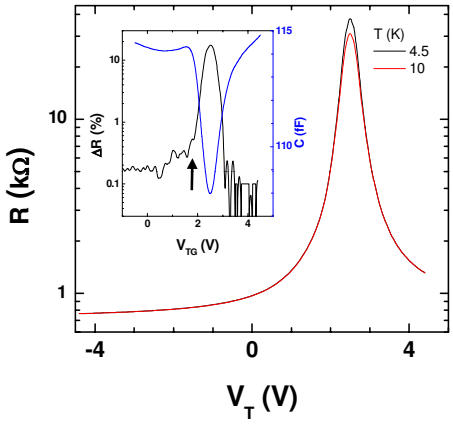

FIG. 4. The resistance at $T = 4.5$ and 10 K. The insulating nature of the low density state is clearly visible. Inset: comparison between capacitance and the percent change in resistance between 10 K and 4.5 K ($\Delta R = (R(T = 4.5\text{K}) - R(T = 10\text{K}))/R(T = 4.5\text{K})$). The capacitance shows no singular behavior at the mobility edge, which is marked by the arrow.

[1] A. K. Geim and K. S. Novoselov. Nature Materials, **6** (2007) 183.
[2] G. Giovannetti, *et al.*, Phys. Rev. B, 76 (2007) 073103.
[3] E. McCann and V. I. Fal'ko, Phys. Rev. Lett., **96** (2006) 086805.
[4] E. V. Castro, *et al.*, Phys. Rev. Lett., **99** (2007), 216802.
[5] E. McCann, Phys. Rev. B, **74**, (2006) 161403.
[6] T. Ohta, A. Bostwick, T. Seyller, K. Horn, and E. Rotenberg, Science, **313** (2006) 951.
[7] Y. Zhang, *et al.*, Nature, **459** (2009) 820.
[8] K. F. Mak, C. H. Lui, J. Shan, and T. F. Heinz, Phys. Rev. Lett., **102** (2009) 256405.
[9] J. B. Oostinga, Nature Materials, **7** (2008) 151.
[10] S. Luryi, Applied Physics Letters, **52** (1988) 501.
[11] S. Ilani, L. A. K. Donev, M. Kindermann, and P. L. McEuen, Nature Physics, **2** (2006) 687.
[12] J. P. Eisenstein, L. N. Pfeiffer, and K. W. West, Phys. Rev. Lett., **68** (1992) 674.
[13] S. C. Dultz and H. W. Jiang, Phys. Rev. Lett., **84** (2000) 4689.
[14] S. Ilani, A. Yacoby, D. Mahalu, and H. Shtrikman, Phys. Rev. Lett., **84** (2000) 3133.
[15] V. S. Khrapai, *et al.*, Phys. Rev. Lett., **99** (2007) 086802.
[16] S. Ilani, A. Yacoby, D. Mahalu, and H. Shtrikman, Science, **292** (2001) 1354.
[17] J. Martin, *et al.*, Nature Physics, **4** (2008) 144.
[18] B. I. Shklovskii and A. L. Efros, *Electronic Properties of Doped Semiconductors*, Springer, New York, 1984.
[19] J. Nilsson and A. H. Castro Neto, Phys. Rev. Lett., **98** (2007), 126801.
[20] V. V. Mkhitaryan and M. E. Raikh, Phys. Rev. B, **78** (2008) 195409.
[21] T. Taniguchi and K. Watanabe, Journal of Crystal Growth **303** (2007) 525.
[22] Y. Kubota, K. Watanabe, O. Tsuda, and T. Taniguchi, Science, **317** (2007) 932.
[23] C.R. Dean, *et al.*, (2010). *In preparation.*
[24] L. Jiao,*et al.*, Nano Letters, **9** (2009) 205.
[25] D. A. Abanin and L. S. Levitov, Science, **317** (2007), 641–643.
[26] J. R. Williams, L. DiCarlo, and C. M. Marcus, Science, **317** (2007) 638.
[27] B. Özyilmaz, *et al.*, Phys. Rev. Lett., **99** (2007) 166804.

[28] D. B. Farmer, *et al.*, Nano Letters, **9** (2009) 4474.
[29] S. V. Kusminskiy, J. Nilsson, D. K. Campbell, and A. H. Castro Neto, Phys. Rev. Lett., **100** (2008), 106805.
[30] F. Borghi, M. Polini, R. Asgari, and A. H. MacDonald, *Private communication.*